RESEARCH ARTICLE

Dissociation of Innate Immune Responses in Microglia Infected with *Listeria monocytogenes*

Elisabet Frande-Cabanes,[1] Lorena Fernandez-Prieto,[1,2] Ricardo Calderon-Gonzalez,[1,2] Estela Rodríguez-Del Río,[1] Sonsoles Yañez-Diaz,[1,3] Monica López-Fanarraga,[2] and Carmen Alvarez-Domínguez[1]

Microglia, the innate immune cells of the brain, plays a central role in cerebral listeriosis. Here, we present evidence that microglia control *Listeria* infection differently than macrophages. Infection of primary microglial cultures and murine cell lines with *Listeria* resulted in a dual function of the two gene expression programmes involved in early and late immune responses in macrophages. Whereas the bacterial gene *hly* seems responsible for both transcriptional programmes in macrophages, *Listeria* induces in microglia only the tumor necrosis factor (TNF)-regulated transcriptional programme. *Listeria* also represses in microglia the late immune response gathered in two clusters, microbial degradation, and interferon (IFN)-inducible genes. The bacterial gene *actA* was required in microglia to induce TNF-regulated responses and to repress the late response. Isolation of microglial phagosomes revealed a phagosomal environment unable to destroy *Listeria*. Microglial phagosomes were also defective in several signaling and trafficking components reported as relevant for *Listeria* innate immune responses. This transcriptional strategy in microglia induced high levels of TNF-α and monocyte chemotactic protein-1 and low production of other neurotoxic compounds such as nitric oxide, hydrogen peroxide, and Type I IFNs. These cytokines and toxic microglial products are also released by primary microglia, and this cytokine and chemokine cocktail display a low potential to trigger neuronal apoptosis. This overall bacterial strategy strongly suggests that microglia limit *Listeria* inflammation pattern exclusively through TNF-mediated responses to preserve brain integrity.

GLIA 2014;62:233–246

Key words: listeriosis, microglia, neuronal cell death, cytokines, macrophages

Introduction

Listeria monocytogenes (LM) is a bacterial pathogen with tropism for human nervous tissue. Listeriosis can be a life-threatening disease causing severe meningitis, encephalitis, and brain abscess in pregnant women, neonates, elderly, and immunocompromised individuals. Some murine models have shown that invasion of the central nervous system (CNS) by LM is facilitated by infected bone-marrow-derived monocytes that adhere to activated brain endothelial cells and accumulate in brain vessels to invade the brain parenchyma (Join-Lambert et al., 2005; Oeverman et al., 2010).

Several cell types have been identified as potential targets of LM in the brain, for example, epithelial cells from choroid plexus, ependymal cells, macrophages, microglia, and neurons (Schlüter et al., 1999). Acute cerebral listeriosis is accompanied by hippocampal neuronal apoptosis (Schlüter et al., 1998). It is known that virulence factors participating in nonlethal infection models also contribute to fatal CNS infection

View this article online at wileyonlinelibrary.com. DOI: 10.1002/glia.22602

Published online December 6, 2013 in Wiley Online Library (wileyonlinelibrary.com). Received Feb 10, 2013, Accepted for publication Nov 5, 2013.

Address correspondence to Carmen Alvarez-Dominguez, Grupo de Genómica, Proteómica y Vacunas, Instituto de Formación e Investigación Marqués de Valdecilla (IFIMAV), Avda. Cardenal Herrera Oria, s/n. 39011 Santander, Spain. E-mail: calvarez@humv.es

From the [1]Grupo de Genómica, Proteómica y vacunas, Instituto de Investigación y Formación Marqués de Valdecilla (IFIMAV), Primera Planta-Laboratorio 124, Avda. de Cardenal Herrera Oria, s/n, 39011, Santander, Spain; [2]Departamento de Biología Molecular, Facultad de Medicina, Universidad de Cantabria-IFIMAV, 39008, Santander, Spain; [3]Servicio de Dermatología, Hospital Universitario Marqués de Valdecilla, 39008, Santander, Spain.

Elisabet Frande-Cabanes and Lorena Fernandez-Prieto contributed equally to this work.

Additional Supporting Information may be found in the online version of this article.

(Schlüter et al., 1998, 1999). In this regard, the *hly*-encoded listeriolysin O (LLO) is a pore-forming toxin and the main virulence factor that allows LM to escape from phagosomes. Another virulence factor is the protein encoded by *actA* gen, ActA, a polarized cell-surface protein responsible for LM intracellular motility through interactions with components of the actin cytoskeleton and also involved in LM cell-to-cell dissemination. Finally, two additional virulence factors participate in the intracellular stage of LM, plcA, and plcB (Schlüter et al., 1998), two phospholipases C encoded by *plcA* and *plcB* genes, respectively, that support LLO to dissolve the phagosomes. However, the effect of all these LM virulence factors in bacterial proliferation differs among cell types being used.

Here, we present a new *in vitro* model for LM infection based on mixed cultures of neurons and glia including microglia, the highly specialized brain resident macrophages. In response to injury, pathogen invasion, or stressful conditions, microglia transform into proliferating cells that migrate and behave as macrophages, producing pro- and anti-inflammatory factors that promote protection and repair functions (Greter and Merad, 2013; Hanisch, 2002). However, microglial activation is also a source of soluble and neurotoxic inflammatory mediators, such as tumor necrosis factor (TNF)-α, nitric oxide (NO), or Type I interferons (IFN-$\alpha\beta$), that cause negative effects on neuronal plasticity, neurogenesis, and contribute to neurodegenerative disorders such as Parkinson's and Alzheimer's diseases (Block et al., 2007; Burguillos et al., 2011; Chao et al., 1992; Kaur et al., 2001), disrupting the delicate balance in the CNS. It is still unclear how subclinical microbiological infections can also interfere with the microglial–neuronal equilibrium and contribute to these neurodegenerative pathologies.

This study investigated a relevant cell target for LM infection, microglia, and its putative role in neuronal apoptosis by using primary microglia. We also performed phagocytosis assays by using the murine microglial cell line BV2 and the murine macrophage cell line J774 and four different LM strains: the pathogenic LM^{WT} and the mutant strains $LM^{\Delta LLO}$, $LM^{\Delta ActA}$, and $LM^{\Delta plcA\Delta plcB}$. Our phagocytic functional studies included analysis of cell surface markers, transcriptional responses with differential displayed microarrays, cytokine measurements, microbicidal mechanisms, and protein composition of isolated phagosomes or postnuclear supernatants (PNS).

Abbreviations

actA	LM gene coding for ActA, a LM protein responsible for actin polymerization
BMDM	bone-marrow derived macrophage
CCL	chemokine CC ligand
CFU	colony forming units
CNS	central nervous system
FITC	fluorescein isothiocyanate
HBE	HEPES buffer with EDTA
hly	LM gene coding for listeriolysin O
H_2O_2	hydrogen peroxide
IFN	interferon
IL	interleukin
i.p.	intra-peritoneal
LLO	listeriolysin O protein
LM	*Listeria monocytogenes*
LPS	lipopolysaccharide
MCP	monocyte chemotactic protein
MHC-II	major histocompatibility class II molecules
NEEA	nonessential amino acids
NO	nitric oxide
NOD	nucleotide-binding and oligomerization domain receptor
PI3K	phosphatidylinositol 3 kinase
PE	phycoerithrin
PNS	postnuclear supernatants
TLR	Toll-like receptor
TRITC	tetramethylrodamine B isothiocyanate

Materials and Methods

Animals

We used C57BL/6 mice from our animal facilities at the University of Cantabria. Bone marrow-derived macrophages (BMDMs) were obtained from femurs of 8- to 12-week-old female mice, cultured, and differentiated in Dulbecco's Modified Eagle's Medium supplemented with 20% fetal calf serum, 1 m*M* glutamine, 1 m*M* NEAA, 25 ng/mL macrophage colony-stimulating factor, 50 μg/mL gentamicin, and 30 μg/mL vancomycin for 7 days. Newborn C57BL/6 pups were used to obtain cerebellum for preparation of mixed microglia and subsequent isolation of primary microglial cultures.

Mixed Microglial Cell Cultures, Purified Primary Microglia, and Cell Lines

Microglial cultures have been described previously (Lopez-Fanarraga et al., 2007; Ribes et al., 2010; Scheffel et al., 2012). Detailed procedures for obtaining mixed microglial cell cultures, purified primary microglia, the microglial cell line BV2, and the murine macrophage cell line J774 are described in Supporting Information.

Bacteria

Prof. D.A. Portnoy (University of California. Berkeley, CA) provided *L. monocytogenes* 10403S pathogenic strain (LM^{WT}) and the mutant strains $LM^{\Delta LLO}$, $LM^{\Delta ActA}$, and $LM^{\Delta plcA\Delta plcB}$. GFP-*LM* DH-L1039 (GFP-LM) derived from the 10403S LM strain was a gift from Prof. D.E. Higgins (Harvard Medical School, Boston, MA).

Kinetic Infection Assays

Cell lines, mixed microglial cultures, BMDMs, and purified primary microglia were infected as described in Supporting Information and previously (Carrasco-Marin et al., 2009, 2011). Replication indexes (RIs) were calculated as previously reported (Alvarez-Dominguez and Stahl, 1999; Alvarez-Dominguez et al., 2000; Carrasco-Marin et al., 2009, 2012; Del Cerro-Vadillo et al., 2006; Prada-Delgado et al., 2001).

Phagosome and Endosome Isolation and Protein Composition Analysis

BV2 and J-774 cells were infected with LM strains (LM^{WT}, $LM^{\Delta LLO}$, $LM^{\Delta ActA}$, or $LM^{\Delta plcA\Delta plcB}$ mutants) for 20 min (10:1;

bacteria:cell ratio) and phagosomal fractions were isolated from thawed PNSs as previously described (Alvarez-Dominguez et al., 1999; Carrasco-Marin et al., 2009, 2011, 2012; Del Cerro-Vadillo et al., 2006; Prada-Delgado et al., 2001). Endosomes form noninfected BV2 and J-774 cells were obtained as described (Del Cerro-Vadillo et al., 2006; Prada-Delgado et al., 2001; Rodriguez-Del Rio et al., 2011) and detailed in Supporting Information. Endosomal fractions were used as control vesicles to standardize basal levels for protein composition analysis (CONT) (Rodriguez-Del Rio et al., 2011).

Comparative Analysis of Phagosomal and Cytosolic Bacteria

J-774 and BV2 cells were infected with LM, and phagosomes were isolated as described above. Cytosol was prepared (Carrasco-Marin et al., 2009, 2011) and percentages of phagosomal and cytosolic bacteria were calculated as described in Supporting Information.

Fluorescence Label, Confocal Microscopy, and Apoptosis

Cells used for immunocytochemistry were fixed in 3% paraformaldehyde. Fluorescence labeling, confocal microscopy, and apoptosis studies of HN9 neurons were performed as previously described (Carrasco-Marin et al., 2011).

Measurement of NO and Hydrogen Peroxide (H_2O_2) Production

J-774 cells, BV2 cells, BMDMs, or purified primary microglia were infected with LM and assayed for NO production or H_2O_2 as previously reported (Alvarez-Dominguez and Stahl, 1999; Alvarez-Dominguez et al., 2000).

Flow Cytometry Analysis

After infection with different LM mutants, proinflammatory cytokine production was measured in cultured supernatants of J-774 cells, BV2 cells, BMDMs, or purified primary microglia by using a CBA proinflammatory kit (BD Life Sciences) (Carrasco-Marin et al., 2009, 2011; Del Cerro-Vadillo et al., 2006). J-774 cells, BV2 cells, BMDMs, or purified primary microglia were incubated in microtiter plates at a density of 2×10^6 cells/mL with medium alone or with medium containing 2×10^7 CFU/mL of LM for 1 h without antibiotics, followed by 24 h incubation in complete medium. Cells were centrifuged and half of the supernatant volume was harvested and stored at –80°C until fluorescence-activated cell sorting (FACS) analysis was performed. Samples were analyzed in triplicate and results are shown as mean ± SD of two separate experiments. We also used FACS analysis for evaluation of cell surface markers in J-774 cells, BV2 cells, BMDMs, or purified primary microglia: CD45-fluorescein isothiocyanate (FITC), CD14-FITC, F4/80-PE, IA^d-APC (MHC-II in J-774 cells), or IA^b-APC (MHC-II of in BV2 cells, BMDMs, and primary microglia), and CD11b-APC.

Transcriptional Expression of Microglial Cells

BV-2 cells were infected with different LM strains and after RNA isolation we performed differential microarrays using the Affimetrix GeneChip MOE430A2.0 that evaluates 22.626 mouse genes (Carrasco-Marin et al., 2012). Microarray analyses were deposited in NCBI Gene Expression Omnibus (Alvarez, 2011) and accessible through GEO Series accession number GSE32505 (http://www.ncbi.nlm.nih.gov/geo/query/acc.cgi?acc=GSE32505). Results of the differential microarrays are expressed as signal log ratio (SLR). All final values were subtracted from values of basal controls that corresponded to noninfected cells (NI) detailed in Supporting Information as reported (Carrasco-Marin et al., 2012).

Statistical Analysis

For statistical analysis, the Student's t test was applied. $P \leq 0.05$ was considered significant using GraphPad for graphic presentation.

Ethics Statement

This study was carried out in strict accordance with the recommendations in the Guide for the Care and Use of Laboratory Animals of the Spanish Ministry of Science, Research and Innovation. The Ethical Committee of Animal Experiments of the University of Cantabria approved this protocol (Permit Number: 2009/12) that follows the Spanish legislation (RD 1201/2005). All surgery was performed under sodium pentobarbital anesthesia and all efforts were performed to minimize suffering.

Results

LM Invades Mainly Microglial Cells

We first investigated two potential cell targets of LM^{WT} in the CNS by establishing an *in vitro* infection model based on primary cultures of murine neurons that contained ~95% neurons, 2% microglial cells, and some other types of glia (Lopez-Fanarraga et al., 2007). This mixed culture system allowed us to analyze the interactions between these two cell populations. As shown in Fig. 1A,B, LM^{WT} (green channel) effectively infected primary microglia (red channel), but it was virtually absent in neurons (blue channel). We also observed viable bacteria in the cytosol nucleating actin comet tails (Fig. 1A inset). Infected microglia exhibited a highly reactive morphology visualized with TRITC-phalloidin that stains actin filaments (Fig. 1A) and expressing macrophagic markers such as F4/80 (red channel) (Fig. 1B). We found virtually no bacteria outside the microglia (inset in Fig. 1B shows a lower magnification image). Therefore, this hippocampal mixed culture system strongly suggested that microglia were the primary cells for LM^{WT} infection because they were more active capturing bacteria than neurons. Quantification of the percentages of infected microglia over 10 different experiments performed in triplicate showed that 99% of microglia were infected with LM and barely 0.01% neurons contained bacteria (Fig. 1A,B).

Microglia Control LM Infection Different from Macrophages

Next, we performed growth kinetic analysis of LM^{WT} within these hippocampal mixed cultures (Mixed-MG in Fig. 1D)

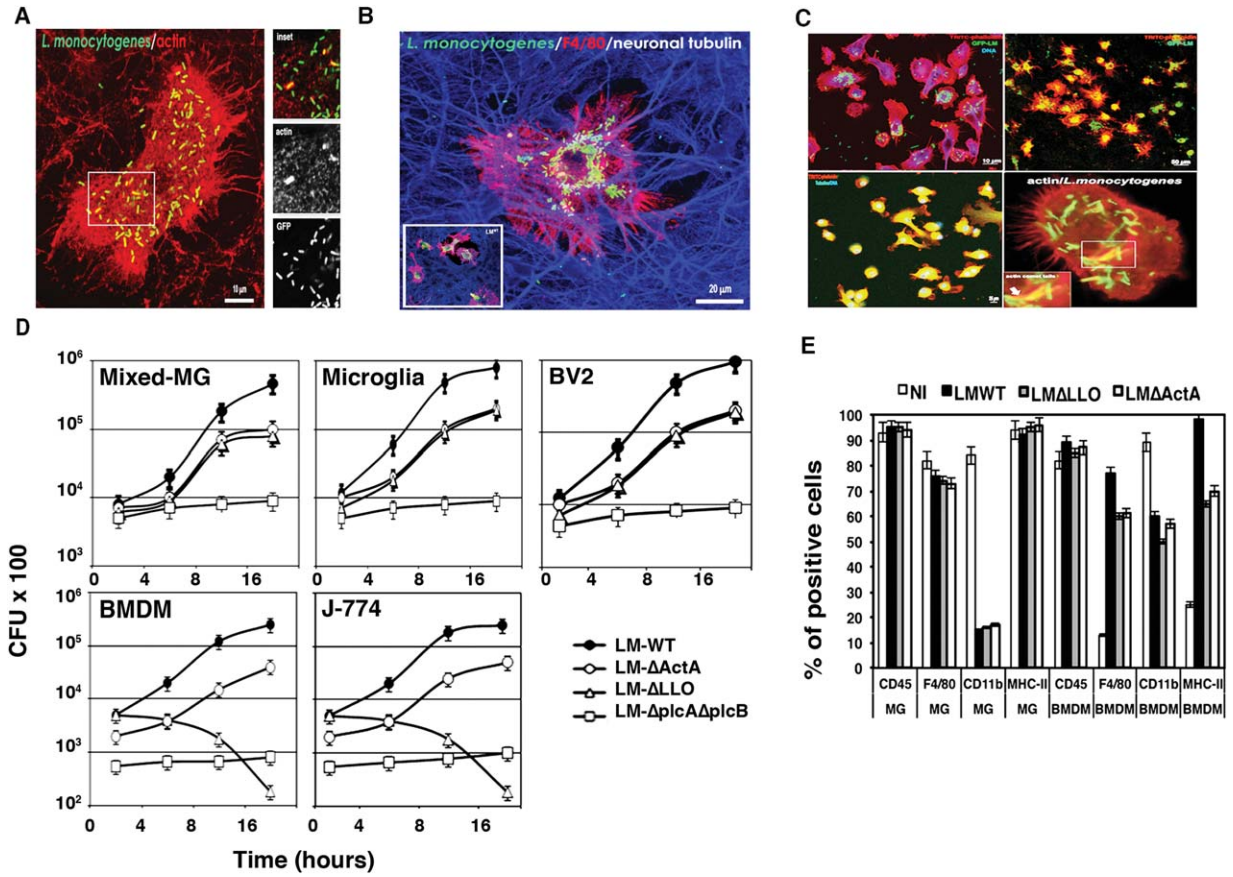

FIGURE 1: ***Listeria monocytogenes*** **invade mainly microglia. (A) Confocal microscopy projection image of mixed microglial cultures infected with LM. GFP-LM (green channel) invaded microglial cells showing actin filaments (red channel). Inset represents single confocal *Z*-plane images that showed actin (red channel) encapsulation of GPF-LM in murine microglia. Colocalization of GFP-LM and actin (yellow fluorescence) showed actin-comet tails. (B) Confocal microscopy projection image of murine mixed microglial cultures infected with GFP-LM. Microglial cells labeled with F4/80 (red channel) were massively infected with GFP-LM (green channel) while surrounding neurons labeled with antitubulin β3 antibody (blue channel) did not show intracellular bacteria. Inset corresponds to a lower magnification field. (C) Purified primary microglia were isolated from mixed microglial cultures at day 7 by shaking at 200 times/min for 30 min and cells in supernatants replated in 24-well with cover-slips for confocal images. Quality of the microglia preparation was observed (lower image) by confocal microscopy staining actin filaments with TRITC-phalloidin (red channel) and tubulin (green channel), intracellular colocalization of red and green fluorescences is a feature of microglia, while in neurons actin and microtubule filaments do not colocalize. All these microglia preparations were $CD11b^{+}F4/80^{+}IA^{b+}CD45^{+}$ with 90% double positive $CD11b^{+}CD45^{+}$ by FACS, reflecting their microglia origin and purity. Next, we infected these microglia with GPF-LM^{WT} (upper images) for 2 h and stained actin filaments with TRITC-phalloidin and nuclei with Hoechst. Bars scale were 10 μm for left upper, 50 μm for right upper, and 25 μm for lower images. Colocalization of GFP-LM^{WT} and actin (yellow fluorescence) showed actin-comet tails in the cytosol (inset represents an enlarged image of actin-comet tails) (lower right image). (D) Kinetic analysis of murine mixed microglial primary cultures, BMDMs, primary purified microglia, BV2 and J-774 cells infected with different LM strains (LM^{WT}, $LM^{\Delta LLO}$, $LM^{\Delta ActA}$, or $LM^{\Delta plcA\Delta plcB}$). Results are expressed as CFU (mean ± SD) obtained with triplicate samples from three independent experiments (main differences are always observed between LM^{WT} and $LM^{\Delta LLO}$ and $LM^{\Delta plcA\Delta plcB}$ results, $P < 0.05$). (E) Primary purified microglia or BMDMs were infected with different LM strains (ratio 10:1 of bacteria: cell) or noninfected (NI) for 2 h, detached from plates, washed several times and surface stained with the following FITC or PE- labeled antibodies: CD45-FITC, CD14-FITC, F4/80-PE, and anti-IA^{b}-APC or anti-IA^{d}-APC. Samples were acquired using FACSCanto flow cytometer and percentages of positive cells for each antibody are shown. Results are expressed as the mean ± SD of triplicates ($P < 0.05$).**

and observed a characteristic exponential proliferation of 4 h duration that ended in a plateau phase of growth at 16 h post-infection, similar to LM^{WT} kinetics in bone-marrow macrophages (BMDMs) (LM^{WT} plots in Fig. 1D) (Alvarez-Dominguez and Stahl, 1999; Carrasco-Marin et al., 2009, 2011, 2012; Del Cerro-Vadillo et al., 2006; Prada-Delgado et al., 2001). We also used different LM mutant strains with known gene deletions relevant for specific LM intracellular stages: *hly*-deficient ($LM^{\Delta LLO}$), *actA*-deficient ($LM^{\Delta ActA}$), or *plcA* and *plcB*-deficient mutants ($LM^{\Delta plcA\Delta plcB}$) to analyze their role in LM growth in microglia. Although LM^{WT}, $LM^{\Delta LLO}$, and $LM^{\Delta ActA}$ showed characteristic exponential growth, the $LM^{\Delta plcA\Delta plcB}$ strain did not replicate in microglial mixed cultures (Fig. 1D). Next, we purified primary microglia from our

TABLE 1: Phagocytic Functions of Microglia and Macrophages

	Uptake[b]		Replication indexes[c]	
Bacteria[a]	Microglia	BMDM	Microglia	BMDM
LM^{WT}	18130 ± 359	6020 ± 113	80 ± 6	48 ± 6
$LM^{\Delta LLO}$	18100 ± 521	6038 ± 151	32 ± 4	0.1 ± 0.05
$LM^{\Delta ActA}$	18230 ± 389	6025 ± 132	38 ± 6	30 ± 2
$LM^{\Delta plcA\Delta plcB}$	18175 ± 428	6090 ± 144	1 ± 0.04	0.5 ± 0.5

[a]Different LM strains were used for infection of microglia and BMDM as described in Methods.
[b]Cells were infected with [^{35}S]-labeled LM strains for 45 min. Cells were washed and radioactivity associated with cell lysates (CPM) was quantified in a $\beta-$counter as the amount of bacterial uptake by microglia. Results are expressed as cpm of internalized bacteria (mean ± SD) (mean differences are observed between BMDM and microglia results, $P < 0.05$).
[c]RIs were calculated as the ratio of the number of CFU at 16 h divided by the amount of CFU at 0 h. This parameter was considered as an indicator of bacterial growth. Results are expressed as CFU (mean ± SD) (main differences are always observed between LM^{WT} and $LM^{\Delta LLO}$ and $LM^{\Delta plcA\Delta plcB}$ results, $P < 0.05$).

microglial mixed cultures and compared the data with BMDMs (Carrasco-Marin et al., 2011, 2013). Quality of the microglia preparation was observed by confocal microscopy staining of actin filaments with TRITC-phalloidin (red channel) that colocalize with tubuline (green channel) (lower left image in Fig. 1C). Intracellular colocalization of actin and tubuline is a feature of microglia, while neurons actin and microtubule filaments do not colocalize. Purified primary microglia infected with LM^{WT} present high numbers of bacteria in the cytosol (upper images in Fig. 1C), nucleate actin filaments (lower right image in Fig. 1C and inset) and show robust exponential growth of LM^{WT}, $LM^{\Delta LLO}$, or $LM^{\Delta ActA}$ strains (Microglia plot in Fig. 1D). All microglia preparations were $CD11b^+F4/80^+IA^{b+}CD45^+$ before LM infection (NI bars in Fig. 1E) with 90% double positive $CD11b^+CD45^+$ cells by FACS, reflecting their microglia origin and purity (Greter and Merad, 2013; Scheffel et al., 2012). Interestingly, microglia decreased significantly $CD11b^+$ expression after LM infection and showed no modification on F4/80 and IA^b markers (MG bars in Fig. 1E). BMDMs preparations were $CD11b^+CD45^+$ and become double positive $F4/80^+IA^{b+}$ cells only after LM infection (BMDMs bars in Fig. 1E).

Detailed analysis of phagocytic functions indicated that microglia internalized three-fold higher numbers of bacteria than BMDMs (Uptake data in Table 1). We also examined the intracellular bactericidal capacities of microglia and BMDMs (Carrasco-Marin et al., 2009, 2012; Del Cerro-Vadillo et al., 2006). In BMDMs (Table 1), LM^{WT} and $LM^{\Delta ActA}$ showed bacterial RI >25, indicating rapid LM proliferation (Alvarez-Dominguez et al., 2000; Carrasco-Marín et al., 2011, 2013). BMDMs infected with $LM^{\Delta LLO}$ or $LM^{\Delta plcA\Delta plcB}$ strains showed RI ≤1. In microglia, LM^{WT}, $LM^{\Delta LLO}$, and $LM^{\Delta ActA}$ showed RI >25 and only $LM^{\Delta plcA\Delta plcB}$ mutants showed RI = 1. $LM^{\Delta LLO}$ behaved as a virulent strain in microglia, suggesting that LLO might not be required for phagosomal disruption.

We observed similar results as above using the microglial cell line BV2 (Blasi et al., 1990; Pokock and Liddel, 2001) and the macrophage cell line J774 (Carrasco-Marin et al., 2009, 2011, 2012; Prada-Delagado et al., 2001). BV2 and J774 cells were double positive $CD11b^+CD45^+$ cells and show same differences in F4/80 and IA^b/IA^d markers as microglia and BMDMs (Fig. S1, panel A in Supp. Info.). BV2 cells also showed decreased $CD11b^+$ expression and no modification of F4/80 and IA^b markers after LM infection. Wild-type LM and *hly*- and *actA*-deficient mutants (LM^{WT}, $LM^{\Delta LLO}$, and $LM^{\Delta ActA}$, respectively) showed exponential growth in BV2 cells (BV2 plot in Fig. 1D). However, $LM^{\Delta LLO}$ strain showed no intracellular growth in J774 cells (J774 plot in Fig. 1D) (Carrasco-Marin et al., 2009; Join-Lambert et al., 2005). Similarly, uptake of different LM strains in BV2 was three-fold higher than in J774 cells. We also observed that in BV2, LM^{WT}, $LM^{\Delta LLO}$, and $LM^{\Delta ActA}$ showed bacterial RI >25 (Fig. S1, panel B and C, respectively, in Supp. Info.). Therefore, we concluded that LLO and ActA proteins encoded by *hly* and *actA* genes, were not relevant for LM intracellular growth in all sources of microglia, despite being required for LM proliferation in different macrophages (Carrasco-Marin et al., 2009, 2011, 2012; Del Cerro-Vadillo et al., 2006; Join-Lambert et al., 2005). All together, these data suggested that microglia had a lower bactericidal potential than macrophages.

We next examined the intracellular distribution of LM in BV2 cells by using a technique, described in J774 cells, that quantified viable bacteria in isolated phagosomal and cytosolic fractions (Alvarez-Dominguez et al., 1999; Carrasco-Marin et al., 2009, 2011, 2012). LM^{WT}, $LM^{\Delta LLO}$, and $LM^{\Delta ActA}$ mutants in BV2 cells showed a dominant cytosolic localization

TABLE 2: Subcellular Compartments for Pathogenic and Mutants Strains of LM in BV2 and J-774 cells

	Phagosomal (%)		Cytosolic (%)	
Bacteria[a]	BV2-microglia	J-774-MØ	BV2-microglia	J-774-MØ
LM^{WT}	20 ± 1	30 ± 3	80 ± 6	70 ± 6
$LM^{\Delta LLO}$	38 ± 5	100 ± 5	62 ± 4	0 ± 0.5
$LM^{\Delta ActA}$	20 ± 3	30 ± 3	80 ± 6	70 ± 2
$LM^{\Delta plcA\Delta plcB}$	90 ± 4	75 ± 4	10 ± 4	25 ± 0.5

[a]BV2 and J-774 cells were infected for 2 h with pathogenic LM^{WT} and $LM^{\Delta LLO}$, $LM^{\Delta ActA}$ or $LM^{\Delta plcA\Delta plcB}$ at a 10:1 (cell:bacteria) ratio. Phagosomal and cytsolic fractions were purified from PNS (30 μg), and solubilized. Viable LM was quantified (CFU) to calculate the percentages of phagosomal and cytosolic bacteria. Results are expressed as percentages of total internalized CFU in PNS (mean ± SD). CFU values for PNS at 0 h were in J-774: 6.5 ± 0.03 for LM^{WT}, 32.5 ± 0.1 for $LM^{\Delta LLO}$, 63.7 ± 0.01 for $LM^{\Delta ActA}$ and 7.0 ± 0.03 for $LM^{\Delta plcA\Delta plcB}$. CFU values for PNS at 0 h were in BV2: 6.5 ± 0.03 for LM^{WT}, 32.5 ± 0.1 for $LM^{\Delta LLO}$, 63.7 ± 0.01 for $LM^{\Delta ActA}$, and 7.0 ± 0.03 for $LM^{\Delta plcA\Delta plcB}$.

with only 20–38% of bacteria in phagosomes (Table 2), whereas the $LM^{\Delta plcA\Delta plcB}$ mutant showed a dominant phagosomal distribution. We also confirmed the intracellular distribution of the different LM strains (Supp. Info. Fig. S2) and the colocalization of actin filaments with cytosolic LM using confocal microscopy (Arrows in Fig. S3 of Supp. Info.).

LM actA Gene Regulates TNF-Induced Immune Gene Expression in Microglia that Transforms Phagosomes into Deficient Innate Immune Platforms

Only cytosolic LM induces innate immune transcriptional responses in macrophages (Carrasco-Marin et al., 2011; Herskovits et al., 2007; Leber et al., 2008; MacCaffrey et al., 2004). Here, we analyzed the differential expression of genes included on the Affimetrix GeneChip MOE430A2.0 in BV2 cells after infection with cytosolic LM strains (pathogenic LM^{WT} as well as the attenuated $LM^{\Delta LLO}$ and $LM^{\Delta ActA}$) as compared with basal levels of noninfected cells. We used BV2 cells using a previously reported strategy for J774 cells infected with LM that combines transcriptional analysis and protein composition of the phagosomal platform (Carrasco-Marin et al., 2012). We analyzed the transcriptional data using an approach focused on functional clusters involved in macrophages innate immunity (Fig. 2A) (Carrasco-Marin et al., 2012; Herskovits et al., 2007; Leber et al., 2008; McCaffrey et al., 2004) (the complete bioinformatics approach is described in Fig. S4, panels A and B of Supp. Info.). Our approach selected the 20 highest differentially expressed genes in microglia, sorting them in two transcriptional patterns: a pattern common to macrophages and a pattern specific for microglial immune response (Fig. 2A and Supp. Info. Table S1). The gene expression pattern shared by macrophages involved Toll-like receptor (TLR), TNF, phosphoinositide 3-kinase (PI3K), and nuclear factor (NF)-κB signaling routes (Carrasco-Marin et al., 2012; Herskovits et al., 2007; Leber et al., 2008; McCaffrey et al., 2004; Scheffel et al., 2012). The *actA* gene of LM appeared to induce the expression of chemokines/cytokines genes *cxcl2, ccl4*, and *tnf-α*, the transcriptional factor NfkB, and the TLR-associated gene *cd14* (Fig. 2A). The *hly* gene of LM might be important for a minimal part of this signaling route involving the *pi3k* catalytic polypeptide gene (Figs. 2A and S4, Panel C in Supp. Info.). Microglia-specific repression included trafficking regulatory genes of phagosomes (Carrasco-Marin et al., 2012), a lysosomal-autophagy gene and IFN-responsive genes. The *actA* gene of LM was involved in repression of trafficking regulatory genes of phagosomes as *rab14*, lysosomal components as *smpd1, vps16, scarb2*, and *rilp12* (Carrasco-Marin et al., 2012) and the lysosomal-autophagy gene, *atg4b* (Supp. Info. Table S1). While the *hly* gene of LM might be involved in repression of the IFN-responsive genes, the chemokine *ccl5*, the kinase associated with IFN receptors *jak1* and upregulation of the IFN signaling repressor, *socs3* gene. We confirmed most of these transcriptional results by performing a detailed protein composition analysis on highly purified LM phagosomes isolated from microglia and based on the signaling components that were highlighted in the transcriptional response (Fig. 2C). We used the innate immune LM phagosomal platforms recently reported for J774 cells as templates and as protein basal controls, endosomes from noninfected BV2 and J774 cells (CONT lanes in Fig. 2C) (Carrasco-Marin et al., 2012). We included RNA contamination controls that might influence signaling inside the phagosomes and an internal protein loading control in all our phagosomal preparations to verify the quality of microglial phagosomes. Quality of purified microglial phagosomes was as follows: protein yields of ∼1 mg/mL from 1×10^9 starting cells

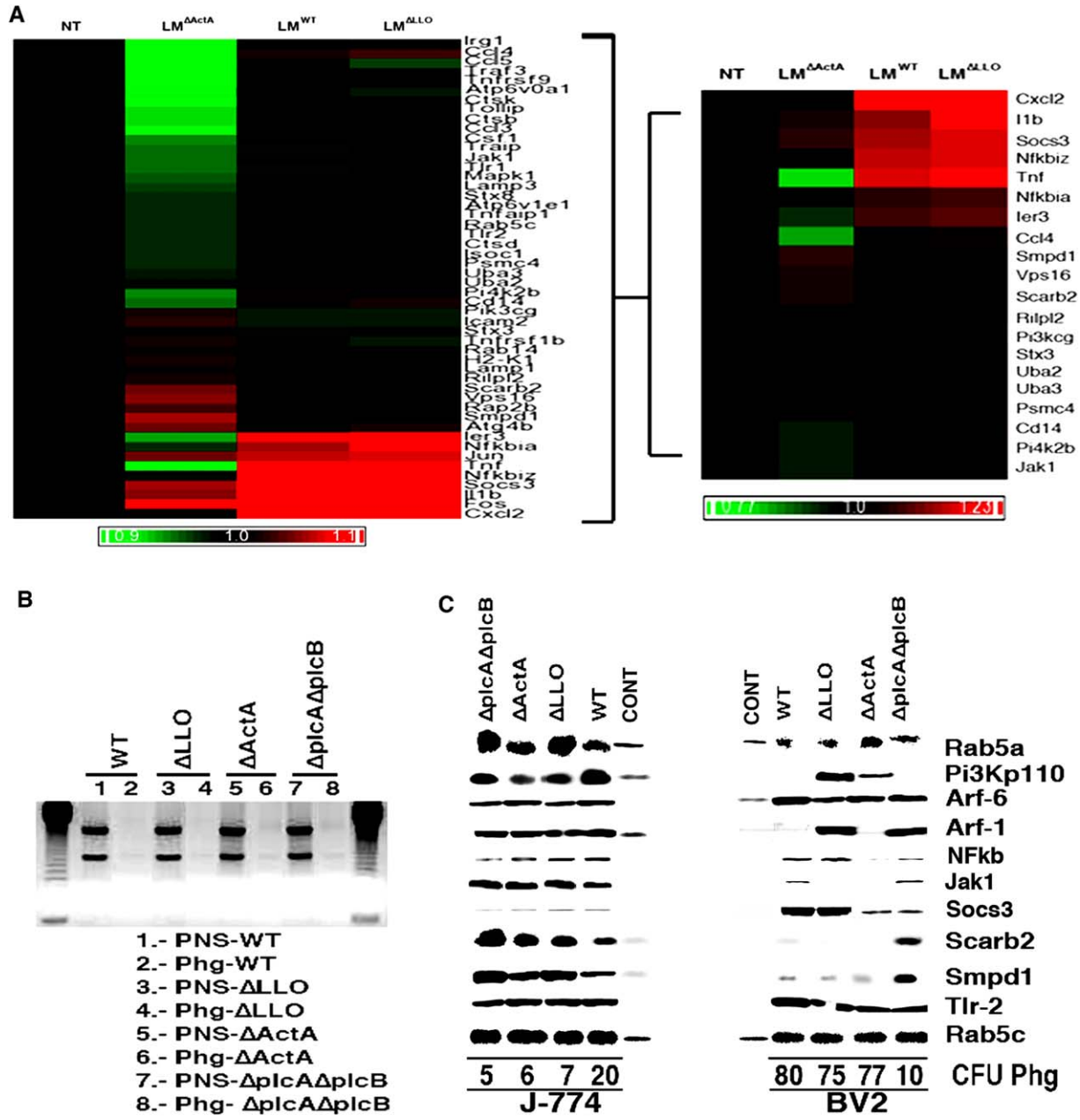

FIGURE 2: LM *actA* gene regulates TNF-mediated immune gene expression in microglia, which transforms phagosomes into deficient innate immune platforms. (**A**) Noninfected (NT) or LM-infected (LM^{WT}, $LM^{\Delta LLO}$, or $LM^{\Delta ActA}$) BV2 cells were used for RNA isolation and differential microarrays. Heat Map presentation of the 20 highest differentially expressed genes representing the LM innate immunity cluster (see Supp. Info. Fig. S3). Colored rows represent expression ratios from ≤ –1.2-fold-change (FC)-repressed genes shown in green to ≥1.2 FC-induced genes shown in red. Black boxes correspond to nondifferentially-expressed genes. (**B**) Examination of RNA quality in phagosomal preparations. By using 1% agarose gel, RNA major bands, a small ~2 kb and a large ~5 kb band, and no fragmented RNA were visualized. In PNSs we observed rRNA (lanes 1, 3, 5, and 7), although no detectable rRNA was observed in phagosomes (lanes 2, 4, 6, and 8). J-774 and BV2 phagosomes usually contain yields of proteins ranging from ~1 mg/mL and 1–3% of RNA contamination. (**C**) Protein and functional analysis of phagosomes and endosomes as basal controls. Western blots of 30 μg per lane of J-774 or BV2 isolated phagosomes containing LM^{WT}, $LM^{\Delta LLO}$, $LM^{\Delta ActA}$, or $LM^{\Delta plcA\Delta plcB}$ or endosomes from noninfected J-774 or BV2 (CONT lanes) showed different relevant proteins, TLR-2, Pi3kp110, NFkB, Jak1, Socs3, Arf-1, Arf-6, and Rab5a, as well as lysosomal markers, Scarb2, and Smpd1. Rab5c was selected as an internal control marker because it showed no variation in J-774 phagosomes and it is also found in endosomes. CFU numbers under western-blot lanes reflected the amount of live bacteria within the phagosomes. [Color figure can be viewed in the online issue, which is available at wileyonlinelibrary.com.]

similar to standard phagosomal purifications in macrophages (Alvarez-Dominguez and Stahl, 1999; Carrasco-Marin et al., 2009, 2011, 2012; Del Cerro-Vadillo et al., 2006; Prada-Delgado et al., 2001), and similar levels of the internal loading control Rab5c (Fig. 2C) (Carrasco-Marin et al., 2012). RNA ranges were lower than those reported in macrophages (Carrasco-Marin et al., 2012) with 1–2% RNA contamination (Supp. Info. Table S2) and a lack of the two rRNA forms, the small ~2 kb and large ~5 kb bands as compared with nonpurified fractions (Fig. 2B). Next, we verified TLR signaling by studying TLR2 protein levels because LM signals through this TLR (Herskovits et al., 2007; Leber et al., 2008; McCaffrey et al., 2004). We observed similar TLR2 levels in microglia and macrophage phagosomes containing the different LM strains, while TLR2 was not detected in endosomes as expected (Fig. 2C). CD14 surface expression in microglia and macrophages infected with LM^{WT} or LM mutants was also comparable (Figs. 1E and S1, panel A in Supp. Info.). We next analyzed PI3K signaling upon protein expression of its p110 catalytic subunit and two components of this pathway: Rab5a that acts upstream and activates the phagosomal oxidase (Carrasco-Marin et al., 2011, 2012; Prada-Delgado et al., 2001), and Arf-1 that acts downstream in the phagocytic cups (Beemiller et al., 2006). LM blocked PI3K signaling in microglia, which involved the LM *hly* gene (Supp. Info. Fig. S4C). However, LM did not inhibit PI3K but activated this kinase signaling in macrophages (Carrasco-Marin et al., 2012; Herskovits et al., 2007; Leber et al., 2008; MacCaffrey et al., 2004). Accordingly, microglial phagosomes containing LM^{WT} and $LM^{\Delta ActA}$ showed low levels of PI3K p110 catalytic subunit, Arf-1, and lower levels of Rab5a than macrophage phagosomes (Fig. 2C). In contrast, microglial phagosomes containing $LM^{\Delta LLO}$ presented high levels of PI3K p110 and Arf-1 and normal levels of Rab5a. We concluded that microglial phagosomes loaded with LM^{WT} and $LM^{\Delta ActA}$ strains contained an inactivated PI3K pathway with LM *hly* gene being involved in PI3K inactivation. LM activates NFkB signaling, which in microglia involved LM *actA* gene. Accordingly, microglia phagosomes containing $LM^{\Delta ActA}$ strains showed no detectable NFkB levels (NFkB lane in Fig. 2C). We also examined the IFN receptor associated kinase Jak1 and the IFN repressor Socs3. Similar to the IFN transcriptional response in macrophages, LM phagosomes show high levels of Jak1 and very low levels of Socs3 (Jak1 and Socs3 lanes in Fig. 2C). LM inactivates IFN transcriptional routes in microglia, which involved LM *hly* gen. Consequently, phagosomes of BV2 cells containing LM^{WT} and $LM^{\Delta LLO}$ strains, showed low or undetectable levels of Jak1 and very high levels of Socs3. Next, we analyzed the lysosomal components repressed in microglia by LM *actA* gene. Similar to the transcriptional response analysis, we observed low levels of two lysosomal components involved in LM innate immunity, Scarb2, and Smpd1 (Fig. 2C) (Carrasco-Marin et al., 2011; Schramm et al., 2008; Utermöhler et al., 2003). Other phagosomal trafficking components such as Arf-6, the PLD-activator, showed normal levels in LM phagosomes from microglia and macrophages (Fig. 2C). Endosomal protein composition validated our analysis since endosomes only contain detectable levels of the trafficking components Rab5a, Rab5c, Pi3Kp110, Arf-6, or Arf-1, as expected. We also verified this complete protein analysis using PNS from purified microglia (data not shown) and obtained same results as with phagosomes of BV2 cells (Fig. 2C). Phagosome composition suggested that LM phagosomes in microglia might not be considered innate immune platforms controlling bacterial viability as in macrophages (Carrasco-Marin et al., 2012). In fact, CFU count inside LM phagosomes from microglia was higher than that observed in LM phagosomes from macrophages (CFU percentages under protein lanes in Fig. 2C).

LM Infection of Microglial Cells Dissociates TNF from IFN Function

Two innate immune signals control LM infection, TNF-mediated genes, and IFN-regulated genes (Carrasco-Marin et al., 2012; Herskovits et al., 2007; Leber et al., 2008; McCaffrey et al., 2004). First, we observed that after LM^{WT} infection, purified primary microglia produced 10-fold higher levels of TNF and 3.5-fold higher levels of the TNF-regulated chemokine CC ligand (CCL)2/monocyte chemotactic protein (MCP)-1 than BMDMs did (Fig. 3A,B). Infection with $LM^{\Delta ActA}$ induced production of basal levels of both cytokines/chemokines in microglia as compared with normal levels in macrophages. Therefore, LM *actA* gene might be involved in TNF production in microglia. Other proinflammatory cytokines such as interleukin (IL)-6 or IL-12 were produced at similar levels in microglia and macrophages infected with LM^{WT}, $LM^{\Delta LLO}$, or $LM^{\Delta ActA}$ strains. IFN-$\alpha\beta$ production was undetectable in microglia infected with pathogenic LM^{WT}, $LM^{\Delta LLO}$, or $LM^{\Delta ActA}$ and at least 100-times lower than in BMDMs. Interestingly, LPS induced similar levels of this cytokine in microglia and BMDMs (white bars in Fig. 3A,B) (Hanisch, 2002; Ribes et al., 2013; Scheffel et al., 2012). Similar results were observed using BV2 and J774 cells (Supp. Info. Table S3).

In macrophages, IFN-mediated genes regulate NO and H_2O_2 production, while TNF signaling controls only NO release (Carrasco-Marín et al., 2012; Cohen et al., 2000; Jun et al., 1993; MacMicking et al., 1997; Prada-Delgado et al., 2001). NO and H_2O_2 are the main microbicidal mechanisms acting in macrophages (Alvarez-Dominguez et al., 2000; MacMicking et al., 1997) and in microglia (Block et al., 2007; Burguillos et al., 2011; Chao et al., 1992; Ribes et al., 2010;

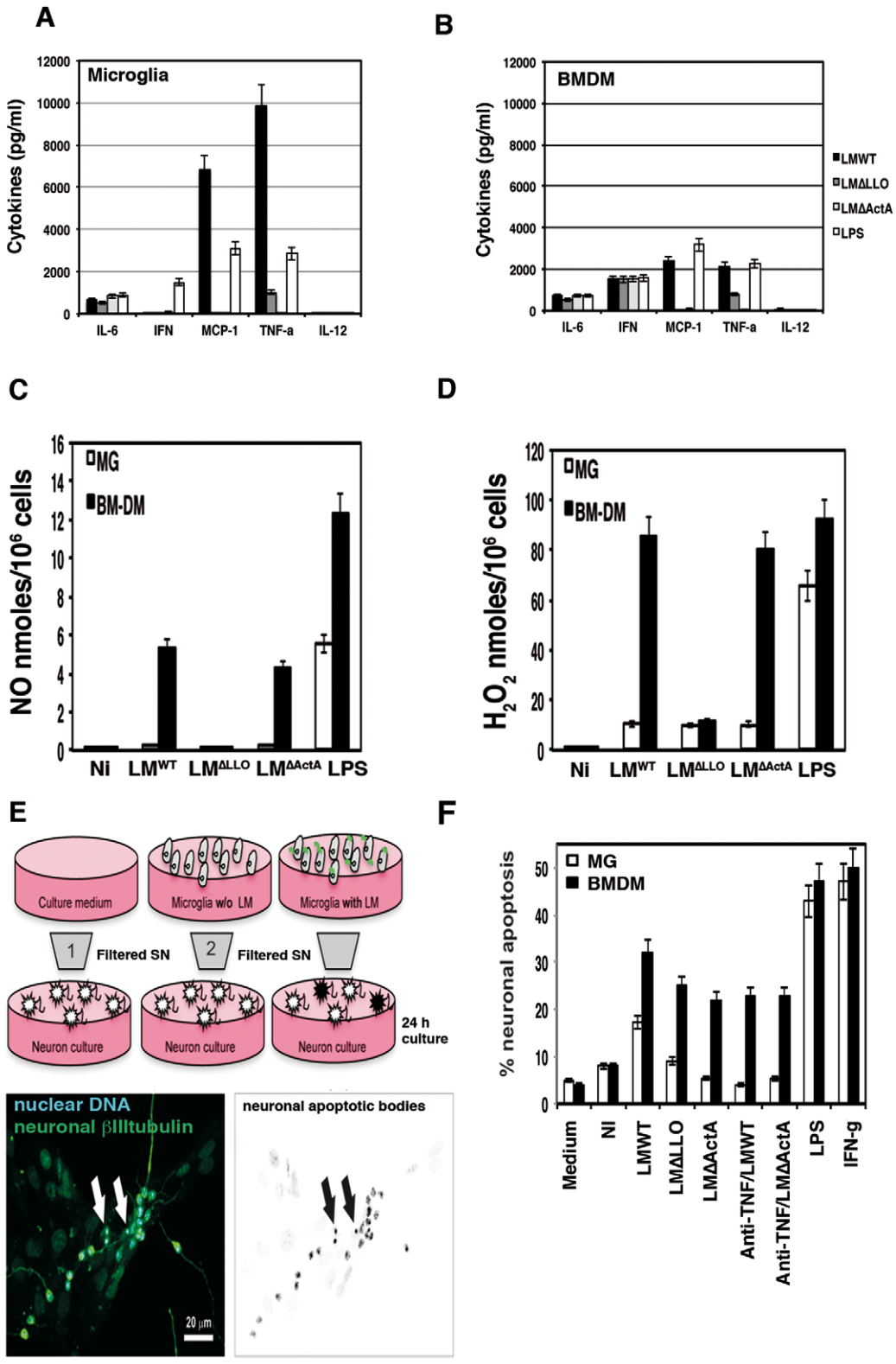

FIGURE 3: Purified primary microglia produces low neurotoxic and microbicidal compounds and limit neuronal apoptosis. (**A**) Purified primary microglia and (**B**) bone-marrow derived macrophages (BMDM) were infected with different mutants or pathogenic LM strains at a ratio of 10: (bacteria: cells). We also included samples incubated with LPS (10 ng/mL). Culture supernatants were collected after 24 h infection in medium containing 50 μg/mL gentamicin to kill extracellular bacteria. Supernatants were filtered before storage at –80°C. Levels of proinflammatory cytokines (MCP-1, TNF-α, IFN-αβ, IL-6, and IL-12) were analyzed by using the CBA kit (Becton Dickinson) and flow cytometry. Results were expressed as cytokine concentration (pg/mL of mean ± SD, $P < 0.05$). (***C***) NO production of BMDMs (black bars) and purified primary microglia (white bars) infected with LM^{WT}, $LM^{\Delta LLO}$, or $LM^{\Delta ActA}$ measured in cell supernatants. Results are expressed as nmol of NO produced by 10^5 cells (mean ± SD, $P < 0.05$) obtained with triplicate samples (main differences are always observed between LM^{WT} and $LM^{\Delta LLO}$ results). (**D**) H_2O_2 production in BMDMs (black bars) and purified primary microglia (white bars) infected with LM^{WT}, $LM^{\Delta LLO}$, or $LM^{\Delta ActA}$. Results are expressed as nmol of H_2O_2 produced per cell (mean ± SD, $P < 0.05$). (***E***) Diagram of the experiment using purified primary microglia (MG) and isolated neurons. Purified primary microglia (MG) were infected with different LM strains for 1 h followed by overnight incubation with complete medium with gentamicin to kill extracellular bacteria. Supernatants were collected and filtered by 0.22 μm filters. (***F***) Isolated neurons were cultured together with a 1/10 dilution of these supernatants for 16 h. In figure, plots of apoptotic neurons are shown after staining and counting using an optical microscope. 50 fields were examined per condition. Results are expressed as percentages (mean ± SD) (mean ± SD, $P < 0.05$) obtained with triplicate samples. [Color figure can be viewed in the online issue, which is available at wileyonlinelibrary.com.]

Schlüter et al., 1999), therefore, we compared the production of these toxic compounds in both cell types. Primary purified microglia infected with LM^{WT} produced lower NO levels than BMDMs did ($P < 0.05$), while infection of microglia with $LM^{\Delta LLO}$ or $LM^{\Delta ActA}$ caused even lower levels ($P < 0.05$) (Fig. 3C). Conversely, BMDMs infected with LM^{WT} or $LM^{\Delta ActA}$ caused high production of NO, and only the $LM^{\Delta LLO}$ strain produced low levels of NO as expected (Boldrick et al., 2001; Cohen et al., 2000; Corr and O'Neil, 2010; Jun et al., 1993; MacMicking et al., 1991; Myers et al., 2003) (Fig. 3C). Moreover, H_2O_2 was undetectable in microglia infected with LM, while macrophages showed high levels after infection with LM mutants (Fig. 3D). Addition of a TLR4 ligand such as lipopolysaccharide (LPS) induced high levels of NO and H_2O_2 in microglia and BMDMs (LPS bars in Fig. 3C,D) (Ribes et al., 2013; Scheffel et al., 2012). BV2 and J774 cells showed similar results (Fig. S5 panel A and B in Supp. Info.). We concluded that TNF and IFN signaling routes regulating NO and H_2O_2 production were dissociated in microglia infected with LM, although not in resting microglia (Hanisch, 2002). However, it is also possible that phagosomes from microglia were not equipped for H_2O_2 production.

In macrophages, expression of MHC-II, F4/80 and CD11b molecules is linked and modulated by IFN genes upon LM infection (Carrasco-Marin et al., 2012; Herskovits et al., 2007; Leber et al., 2008; MacCaffrey et al., 2004). Therefore, dissociation of TNF and IFN mediated responses in microglia such as production of cytokines, NO and H_2O_2 might also correlate with the decrease in the expression of CD11b integrin and the lack of modification in F4/80 and MHC-II levels after LM infection (Figs. 1E and S1, panel A in Supp. Info.). These data also correlates with the induction of a particular subset of microglia after LM infection as reported for TLR-4 activation (Scheffel et al., 2012).

LM-Infected Microglia Avoid Generalized Neuronal Damage

We tested the hypothesis that the microglial strategy after LM infection was focused on reducing neuronal damage. We examined neuronal apoptosis mediated by the products released by microglia infected with LM but without direct contact of neurons with pathogenic LM (Fig. 3E,F). We infected primary purified microglia with pathogenic or LM mutants and collected and filtered the supernatants to eliminate bacteria (Lopez-Fanarraga et al., 2007). Isolated hippocampal neurons were coincubated with a 1/10 dilution of 2 h supernatants for 16 h. We measured nuclear fragmentation as the percentage of apoptotic cells by using either confocal microscopy (Fig. 3E,F) or apoptosis of murine HN9 neurons using FACS analysis with DAPI (Fig. S5, panel D in Supp. Info.). We included two negative controls consisting of culture medium alone (medium bars in Fig. 3F) and cell media with noninfected microglia or BMDMs (NI bars in Fig. 3F). We observed a three-fold increase in apoptosis of primary neurons after incubation with the filtered supernatant of microglia infected with pathogenic LM^{WT} (white bars in Fig. 3F). These apoptotic levels were reverted to basal levels with an anti-TNF antibody and with the supernatant of microglia infected with $LM^{\Delta ActA}$ strain that was unresponsive to TNF antibody (anti-TNF/LMΔActA bars in Fig. 3F). However, neuronal apoptosis increased up to 45–47% after using supernatants of microglia incubated with IFN-γ or with LPS (IFN-g and LPS bars in Fig. 3F). Supernatants from BMDMs infected with LM (black bars in Fig. 3F) showed higher apoptosis (26–38%) than microglia infected with LM (17%). We observed similar results using BV2 and J774 cells (Fig. S5, panel C and D in Supp. Info.).

In summary, these results strongly indicated that the high levels of TNF induced in microglial after LM infection were regulated by the LM *actA* gene and appeared to cause only limited neuronal apoptosis as compared with the apoptosis induced by other stimuli such as LPS or IFN-γ.

Discussion

Microglia are important in cerebral listeriosis to avoid pathogen dissemination into the CNS and preserve brain homeostasis (Dramsi et al., 1998; Drevets et al., 2008; Schlüter et al., 1998, 1999; Sonje et al., 2010; Virna et al., 2006). An excessive inflammatory reaction upon bacterial infection might cause bystander damage, therefore, microglia might count with especial regulatory mechanisms, which may not be necessarily identical to those triggered in innate immune cells such as macrophages (Herskovits et al., 2007; Leber et al., 2008; MacCaffrey et al., 2004).

The present study shows that microglia are relevant target cells for LM in the CNS, and that microglia and macrophages control LM infection differently. Our analysis of the transcriptional response induced by LM indicated that microglial cells triggered a limited innate immune response dominated by two transcriptional programmes. The first expression programme is common to macrophages and microglia and involves TLR, TNF, PI3K, and NF-κB signaling pathways. LM *actA* gene seems to be involved in gene induction of the TLR2-associated molecule involved in LM adhesion *cd14* (Corr and O'Neil, 2010; Herskovits et al., 2007; Leber et al., 2008; MacCaffrey et al., 2004), *NfκB*, *tnf-α* and the chemokines/cytokines genes *cxcl2* and *ccl4*, which are involved in recruiting monocytes. However, we observed similar phagosomal TLR2 levels and CD14 surface expression in microglia and macrophages infected with LM. LM also activates NFkB signaling and bacterial *actA* gene seems to control phagosomal NFkB levels in

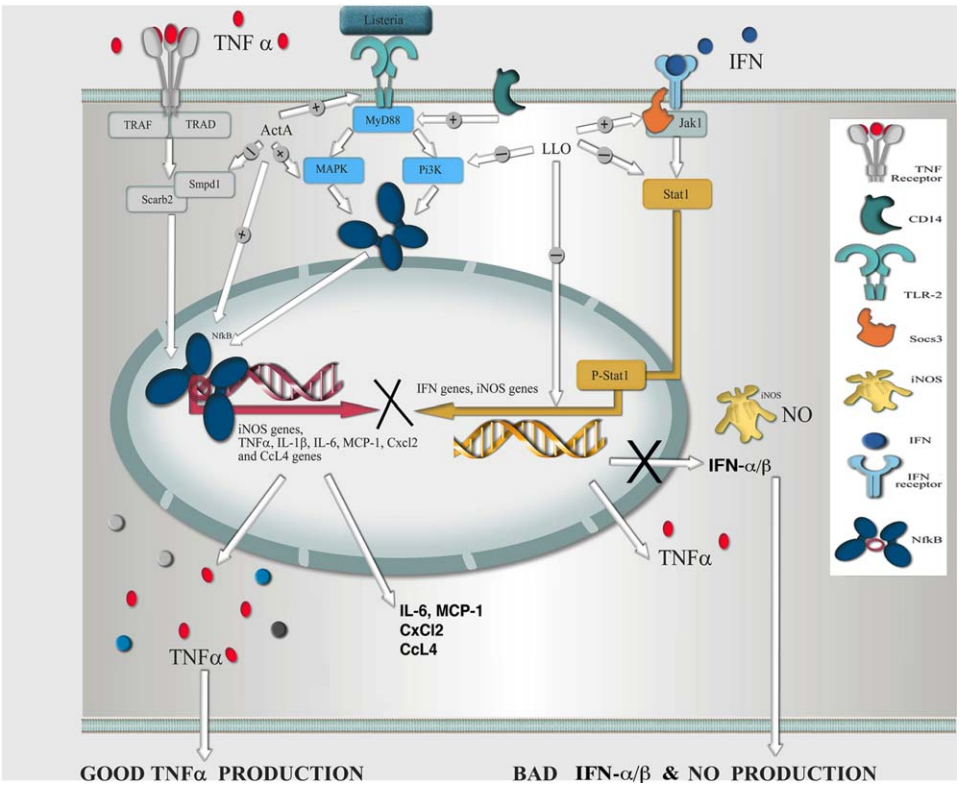

FIGURE 4: Hypothetical model of LM infection in microglia. Pathogenic LM seems to induce in microglia the dissociation of a transcriptional response dominated by innate immunity using three events regulated by the *actA* gene and partially by the *hly* gene: (i) the *actA* gene appears relevant for the induction of early innate responses compiled in three signaling pathways: TLR, TNF, and NF-κB. After bacteria bound to TLR2, induction of mitogen-activated kinase and PI3K seemed to occur with participation of CD14. Subsequent activation of the NF-κB might induce high levels of TNF-α (GOOD TNF-α production in the model) and MCP-1, and CXCL2 and CCL4 chemokines that recruited other monocytes (+ routes). (ii) The *actA* gene also repressed a degradation cluster belonging to late innate responses and characterized by lysosomal genes *smpd1* and *scarb2* (–routes). (iii) The *hly* gene seemed to repress the IFN-responsive gene cluster belonging to late innate responses involving high induction of repressor Socs3 (+ arrow) that blocked the IFN pathway and repressed Jak1, the kinase associated with IFN receptor (–routes). Therefore, production of type I IFNs (i.e., IFN-αβ and NO was decreased (BAD IFN-αβ and NO production in the model) because activation of the iNOS genes appeared compromised. The *hly* gene seemed also important for inhibition of the *pi3kcg* gene that might avoid activation of the phagosomal oxidase (known as *phox*) and block H_2O_2 production. [Color figure can be viewed in the online issue, which is available at wileyonlinelibrary.com.]

microglia. We concluded that bacterial receptor expression or initial steps on phagosomal signaling did not explain the differences between microglia and macrophages.

Measurements of cytokines/chemokines indicated that *actA* gene of LM was responsible for an overproduction of TNF-α and MCP-1/CCL2 in LM-infected microglia. This high production of TNF-α and MCP-1 might recruit other monocytes to the infection site and control pathogen propagation to other cells. These results are in accordance with LM infection of hippocampal mixed cultures, which show bacterial growth only in microglia. Down regulation of migratory markers such as CD11b in microglia infected with LM might also avoid this pathogen dissemination.

The *hly* gene of LM controls part of this early response repressing *pi3kcg*, the catalytic polypeptide gene of PI3K kinase. Consequently, microglial LM phagosomes are deficient in oxidative microbicidal components regulated by PI3K signaling such as PI3K p110, Rab5a, and Arf-1, which might down-regulate the phagosomal oxidase and explain the low levels of microbicidal H_2O_2 that microglia produced after LM infection (Beemiller et al., 2006; Cohen et al., 2000; Jun et al., 1993; Prada-Delgado et al., 2001). The functional analysis indicated that microglia had higher bacterial phagocytic rates but a lower microbicidal potential as compared with macrophages. In fact, LM phagosomes in microglia show much higher CFU values than macrophages suggesting a defective compartment for degradation of bacteria.

This inducible expression programme highlighted two relevant functions of these cells, recruitment of other phagocytes, and activation of innate immune responses to combat intracellular pathogens (Herskovits et al., 2007; Leber et al., 2008; McCaffrey et al., 2004). In contrast, this transcriptional early response in macrophages is induced by phagosome-degraded bacteria and controlled by LM *hly* gene and not by *actA* gene (Herskovits et al., 2007; Leber et al., 2008).

The second gene expression programme is specific for microglia and involves the repression of late innate immune genes classified according to the literature in two functional clusters highly induced in macrophages (Carrasco-Marin et al., 2012; Herskovits et al., 2007; Leber et al., 2008). The first is a degradation cluster mainly characterized by lysosomal trafficking genes and autophagy. The second is a listericidal cluster characterized by IFN-responsive genes involved in production of type I IFN, H_2O_2, and NO (Carrasco-Marin et al., 2012; MacMicking et al., 1997; Myers et al., 2003; Jun et al., 1993). LM *actA* gene seems to be important in the inhibition of the degradation cluster genes participating in organelle fusion, such as syntaxin-3 and syntaxin-8; the specific autophagy gene *atg4b*, which might participate in LM cytosolic degradation (Mostowy et al., 2011; Yin et al., 2009), the lysosomal genes *vps16*, *lamp-1*, and *rilp2* and specially repression of two lysosomal genes involved in LM innate immunity, *scarb2* (Carrasco-Marin et al., 2011) and *smpd1* (Del Cerro-Vadillo et al., 2006; Schramm et al., 2008; Utermöhlen et al., 2003). Therefore, it seems that LM *actA* gene is mandatory in microglia to avoid phagosomal and cytosolic degradation of LM, control late fusion events as well as to up-regulate TNF production (Drevets et al., 2008). We verified that phagosome fusion with late compartments was impaired in microglia but not in macrophages (data not shown). We also confirmed that microglia phagosomes lacked the nonoxidative listericidal components Scarb2 and Smpd1, which are involved in confining LM within the phagosomes (Carrasco-Marín et al., 2011; Schramm et al., 2008; Utermöhlen et al., 2003). Moreover, cytosolic destruction of LM seems to be also partially blocked in microglia, showing a high number of cytosolic bacteria that escaped from phagosomes.

The LM *hly* gene appeared to be relevant for the microglial specific expression programme that represses IFN-responsive genes cluster and avoids amplification of the LM proinflammatory immune response. In fact, IFN-$\alpha\beta$ production is very low in microglia infected with LM. Induction of *socs3* gene in microglia blocked the activation of late immune responses because it is an inhibitor of Type I IFN production (Jun et al., 1993; Herskovits et al., 2007; Leber et al., 2008; MacMicking et al., 1997; McCaffrey et al., 2004; Myers et al., 2003; Utermöhlen et al., 2003). This expression programme also represses *jak1* gene, the kinase associated with IFN receptors. In fact, LM microglial phagosomes showed an inactive IFN pathway since they lack Jak1 and contain high levels of Socs3. These entire genes act as feedback mechanisms to increase the microbicidal machinery of macrophages (Dedoni et al., 2010; Herskovits et al., 2007; Leber et al., 2008; McCaffrey et al., 2004), thus, their repression in microglia after LM infection seemed to favor low levels of toxic H_2O_2. IFN signaling also controls the production of NO in macrophages. Microglia infected with LM released low levels of NO that might not be sufficient to eliminate all cytosolic bacteria. In summary, microglia have poor microbicidal compartments such as phagosomes and cytosol, therefore, it might be difficult for them to generate bacterial ligands for NOD receptors and induce a powerful inflammatory respons(Herskovits et al., 2007; Leber et al., 2008).

This entire transcriptional programme induced by LM infection in microglia seems to dissociate TNF- from IFN-mediated responses (Fig. 4). Cytokine measurements confirmed this hypothesis with an overproduction of TNF-α and MCP-1/CCL2 in LM-infected microglia, but reduced production of Type I IFNs and bactericidal compounds such as H_2O_2 and NO. This dissociation also aims to limit neuronal damage up to a maximum of 17%, because LPS or IFN-γ signals that do not cause this dissociation are more neurotoxic. LM *actA* gene controlled this limited neuronal apoptosis that seems attributed only to microglia TNF-α production. The lack of production of Type I IFNs also limits the acute inflammatory response not recruiting other leukocytes and reduces brain damage (Dedoni et al., 2010; Sonje et al., 2010; Virna et al., 2006; Yin et al., 2009). Our results are contradictory to those reported with a strain of *Listeria*, not previously reported or deposited in data banks, that uses a nervous system model of mixed rat neuronal cultures (Remuzgo-Martinez et al., 2013). Cytokines and gene expression patterns reported by these authors cannot be assigned to microglia since they do not use purified microglia or microglial homogeneous cell lines. The dissociation of LM innate immune responses in microglia that we report in this study seems to correlate with the heterogenicity of microglia responses since LM infection might select a specific microglia population (Scheffel et al., 2012). Moreover, this microglia strategy after infection with LM seems to preserve the delicate brain balance and highlights the role of microglia in preventing microbiological infections that might exacerbate neurodegenerative processes (Dedoni et al., 2010; Dramsi et al., 1998).

Acknowledgment

Grant sponsor: Spanish Secretary of State for Research and Innovation; Grant number: BIO2002-0628, SAF2006-08968, SAF2009-08695, SAF2012-34203; Grant sponsor: IFIMAV; Grant number: API2010/03/SAF2009-08695.

The authors thank M. Garcia-Gil for providing the murine neuron HN9 cells. They are indebted to D. Fernandez (Progenika S.A. Bilbao. Spain) for gene expression analysis and R. Tobes and E. Pareja (Era7 Information Technologies SL. Granada. Spain) for the design of bioinformatics models. They also acknowledge A. San Nicolas-Gomez, L. Bronchalo-

Vicente, and L. Alvarez-Montes for excellent technical assistance and J.C. Zabala (UC Santander) for laboratory support. They also thank S. Ribes, JP Gorvel, and M. Fresno for critical comments on the manuscript, and appreciate A. Tenner's interest in our study.

References

Alvarez-Dominguez C, Stahl P. 1999. Increased expression of Rab5a correlates directly with accelerated maturation of *Listeria monocytogenes* phagosomes. J Biol Chem 274:11459–11462.

Alvarez-Dominguez C, Carrasco-Marín E, López-Mato P, Leyva-Cobián F. 2000. The contribution of both oxygen and nitrogen intermediates to the intracellular killing mechanisms of C1q-opsonized *Listeria monocytogenes* by the macrophage-like IC-21 cell line. Immunology 101:83–89.

Beemiller P, Hoppe AD, Swanson JA. 2006. A phosphatidylinositol-3-kinase dependent signal transition regulates ARF1 and ARF6 during Fcγ-receptor-mediated phagocytosis. PloS Biol 4:e62.

Blasi E, Barluzzi R, Bocchini V, Mazzolla R, Bistoni F. 1990. Inmortalization of murine microglial cells by a v-raf/v-myc carrying retrovirus. J Neuroimmunol 27:229–237.

Block ML, Zecca L, Hong JS. 2007. Microglia-mediated neurotoxicity: Uncovering the molecular mechanisms. Nat Rev Neurosci 8:57–69.

Boldrick JC, Alizadeh AA, Diehn M, Dudoit S, Liu CL, Belcher CE, Botstein D, Staudt LM, Brown PO, Relman DA. 2002. Stereotyped and specific gene expression programs in human innate immune responses to bacteria. Proc Natl Acad Sci U S A 99:972–977.

Burguillos MA, Deierborg T, Kavanagh E, Persson A, Hajji N, Garcia-Quintanilla A, Cano J, Brundin P, Englund E, Venero JL, Joseph B. 2011. Caspase signalling controls microglia activation and neurotoxicity. Nature 472:319–324.

Carrasco-Marin E, Fernández-Prieto L, Rodriguez-Del Rio E, Madrazo-Toca F, Reinheckel T, Saftig P, Alvarez-Dominguez C. 2011. Limp-II links late phagosomal trafficking with the onset of *Listeria monocytogenes* innate immunity: A role in macrophage activation. J Biol Chem 286:3332–3341.

Carrasco-Marín E, Madrazo-Toca F, de los Toyos JR, Cacho-Alonso E, Tobes R, Pareja E, Paradela A, Albar JP, Chen W, Gomez-Lopez MT, Alvarez-Dominguez C. 2009. The innate immunity role of cathepsin-D is linked to Trp-491 and Trp-492 residues of listeriolysin O. Mol Microbiol 72:668–682.

Carrasco-Marin E, Rodriguez-Del Rio E, Frande-Cabanes E, Tobes R, Pareja E, Lecea-Cuello MJ, Ruiz-Sáez M, Madrazo-Toca F, Hölscher C, Alvarez-Dominguez C. 2012. Phagosomes induced by cytokines function as anti-Listeria vaccines: A novel role for functional compartmentalization of Stat-1 and cathepsin-D. J Biol Chem 287:14310–14324.

Chao CC, Hu S, Molitor TW, Shaskan EG, Peterson PK. 1992. Activated microglia mediate neuronal cell injury via a nitric oxide mechanism. J Immunol 149:2736–2741.

Cohen P, Bouaboula M, Bellis M, Baron V, Jbilo O, Poinot-Chazel C, Galiègue S, Hadibi EH, Casellas P. 2000. Monitoring cellular responses to *Listeria monocytogenes* with oligonucleotide arrays. J Biol Chem 275:11181–11190.

Corr SC, O'Neill LA. 2010. *Listeria monocytogenes* infection in the face of innate immunity. Cell Microbiol 11:703–709.

Dedoni S, Olianas MC, Onali P. 2010. Interferon-b induces apoptosis in human SH-SY5Y neuroblastoma cells through activation of JAK-STAT signalling and down-regulation of PI3K/Akt pathway. J Neurochem 115:1421–1433.

Del Cerro-Vadillo E, Madrazo-Toca F, Carrasco-Marín E, Fernandez-Prieto L, Beck C, Leyva-Cobián F, Saftig P, Alvarez-Dominguez C. 2006. A novel non-oxidative mechanism exerted by cathepsin-D controls *Listeria monocytogenes* intracellular growth. J Immunol 276:1321–1325.

Dramsi S, Levi S, Triller A, Cossart P. 1998. Entry of Listeria into neurons occur by cell-to-cell spread: An in vitro model. Infect Immun 66:4461–4468.

Drevets DA, Schawang JE, Dillon MJ, Lerner MR, Bronze MS, Brackett DJ. 2008. Innate responses to systemic infection by intracellular bacteria trigger recruitment of Ly-6Chigh monocytes to the brain. J Immunol 181:529–536.

Greter M, Merad M. 2013. Regulation of microglia development and homeostasis. Glia 61:121–127.

Hanisch UK. 2002. Microglia as a source and target of cytokines. Glia 40: 140–155.

Herskovits AA, Auerbuch V, Portnoy DA. 2007. Bacterial ligands generated in a phagosome are targets of the cytosolic innate immune system. PloS Pathogens 3:e51.

Join-Lambert OF, Ezine S, Le Monnier A, Jaubert F, Okabe M, Berche P, Kayal S. 2005. *Listeria monocytogenes*-infected bone marrow myeloid cells promote bacterial invasion of the central nervous system. Cell Microbiol 7: 167–180.

Jun CD, Kim SH, Soh CT, Kang SS, Chung HT. Nitric oxide mediates the toxoplasmastatic activity of murine microglial cells in vitro. 1993. Immunol Invest 22:487–501.

Kaur C, Hao AJ, Wu CH, Ling EA. 2001. Origin of microglia. Microsc Res Tech 1:2–9.

Leber JH, Crimmins GT, Raghavan S, Meyer-Morse NP, Cox JS, Portnoy DA. 2008. Distinct TLR- and NLR-mediated transcriptional responses to an intracellular pathogen. PloS Pathogens 4:e6.

Lopez-Fanarraga M, Carranza G, Bellido J, Kortazar D, Villegas JC, Zabala JC. 2007. Tubulin cofactor B plays a role in the neuronal growth cone. J Neurochem 100:1680–1687.

MacMicking J, Xie QW, Nathan C. 1997. Nitric oxide and macrophage function. Ann Rev Immunol 15:323–350.

McCaffrey RL, Fawcett P, O'Riordan M, Lee KD, Havell EA, Brown PO, Portnoy DA. 2004. A specific gene expression program triggered by gram-positive bacteria in the cytosol. Proc Nat Acad Sci U S A 101:11386–11391.

Mostowy S, Sancho-Shimizu V, Hamon MA, Simeone R, Brosch R, Johansen T, Cossart P. 2011. P62 and NDP52 proteins target intracytosolic Shigella and Listeria to different autophagy pathways. J Biol Chem 286:26987–26995.

Myers JT, Tsang AW, Swanson JA. 2003. Localized reactive oxygen and nitrogen intermediates inhibit escape of *Listeria monocytogenes* from vacuoles in activated macrophages. J Immunol 171:5447–5453.

Oeverman A, Zurbriggen A, Vandevelde M. 2010. Rhombencephalitis Caused by Listeria monocytogenes in Humans and Ruminants: A Zoonosis on the Rise? Interdiscip Perspect Infect Dis. 2010:632513.

Pokock JM, Liddle AC. 2001. Microglial signalling cascades in neurodegenerative disease. Prog Brain Res 132:555–565.

Prada-Delgado A, Carrasco-Marín E, Peña-Macarro C, Del Cerro-Vadillo E, Fresno-Escudero M, Leyva-Cobián F, Alvarez-Dominguez, C. 2001. Interferon-gamma listericidal action is mediated by novel Rab5a functions at the phagosomal environment. J Biol Chem 276:19059–19065.

Remuzgo-Martinez S, Pilares-Ortega L, Icardo JM, Valdizan EM, Vargas VI, Pazos A, Ramos-Vivas J. 2013. Microglial activation and expression of immune-related genes in a rat ex vivo nervous system model after infection with *Listeria monocytogenes*. Glia 61:611–622.

Ribes S, Ebert S, Regen T, Agarwal A, Tauber SC, Czesnik D, Spreer A, Bunkowski S, Eiffert, Hanisch UW, Hammerschmidt S, Nau R. 2010. Toll-like receptor stimulation enhances phagocytosis and intracellular killing of nonencapsulated *Streptococcus pneumonia* by murine microglia. Infect Immun 78: 865–871.

Rodriguez-Del Rio E, Frande-Cabanes E, Tobes R, Pareja E, Lecea-Cuello MJ, Ruiz-Saez M, Carrasco-Marin E, Alvarez-Dominguez C. 2011. The intact structural form of LLO in endosomes cannot protect against listeriosis. Int J Biochem Mol Biol 2:207–218.

Scheffel J, Regen T, Van Rossum D, Seifert S, Ribes S, Nau R, Parsa R, Harris RA, Boddeke HWGM, Chuang HH, Pukrop T, Wessels JT, Jurgens T, Merkler D, Brück W, Schnaars M, Simmons M, Kettenmann H, Hanisch UK. 2012. Toll-

like receptor activation reveals developmental reorganization and unmasks responder subsets of microglia. Glia 60:1930–1943.

Schlüter D, Back C, Reiter S, Meyer T, Hof H, Deckert-Schluter M. 1999. Immune reactions to *Listeria monocytogenes* in the brain. Immunobiology 201:188–195.

Schlüter D, Domann E, Buck C, Hain T, Hof H, Chakraborty T, Deckert-Schlüter M. 1998. Phosphatidylcholine-specific phospholipase C from *Listeria monocytogenes* is an important virulence factor in murine cerebral listeriosis. Infect Immun 66:5930–5938.

Schramm M, Herz J, Haas A, Krönke M, Utermöhlen O. 2008. Acid sphingomyelinase is required for efficient phago-lysosomal fusion. Cell Microbiol 10: 1839–1853.

Sonje MB, Abram M, Stenzel W, Deckert M. 2010. Listeria monocytogenes (delta-actA mutant) infection in tumor necrosis factor receptor p55-deficient neonatal mice. Microb Pathog 49:186–195.

Utermöhlen O, Karow U, Löhler J, Krönke M. 2003. *Listeria monocytogenes* infection in the face of innate immunity. Severe impairment in early host defense against Listeria monocytogenes in mice deficient in acid sphingomyelinase. J Immunol 170:2621–2628.

Virna S, Deckert M, Lütjen S, Soltek S, Foulds KE, Shen H, Körner H, Sedgwick JD, Schlüter D. 2006. TNF is important for pathogen control and limits brain damage in murine cerebral listeriosis. J Immunol 177:3972–3982.

Yin F, Banerjee R, Thomas B, Zhou P, Qian L, Jia T, Ma X, Ma Y, Iadecola C, Beal MF, Nathan C, Ding A. 2009. Exaggerated inflammation, impaired host defence, and neuropathology in progranulin-deficient mice. J Exp Med 207:117–128.